ACCEPTED MANUSCRIPT

Single- and dual-variant atomic ordering in GaAsP compositionally graded buffers on GaP and Si substrates

R.M. France,[1] M. Feifel,[2] J. Belz,[3] A. Beyer,[3] K. Volz,[3] J. Ohlmann,[2] D. Lackner,[2] and F. Dimroth[2]

[1]National Renewable Energy Laboratory, Golden, CO, 80401, USA
[2]Fraunhofer Institute for Solar Energy Systems ISE, 79110 Freiburg, Germany
[3]Materials Science Center and Faculty of Physics, Philipps-Universität Marburg, Marburg 35032, Germany

Abstract

We investigate the material properties of GaAsP graded buffers on both GaP and Si substrates in order to determine limitations to dislocation glide in GaAsP. Phase separation is not observed in these GaAsP buffers, but $CuPt_B$ atomic ordering is present, and has an impact on the Burgers vector distribution of gliding dislocations. Tellurium surfactant eliminates ordering in GaAsP, allowing control over the glide plane distribution while highlighting the importance of the growth surface and choice of dopant.

The impact of single-variant $CuPt_B$ ordering of GaAsP buffers grown on GaP substrates is investigated by monitoring the threading dislocation density throughout the buffer in sequential steps. The dislocation density rises steadily throughout the graded buffer, implying that factors other than ordering-induced glide plane switches play a dominant role in the final dislocation density. We observe an increase in surface roughness throughout the buffer and speculate that a dislocation nucleation source on the surface has a low activation energy and may lead to increased threading dislocation density.

On Si substrates, the GaAsP buffer displays dual-variant $CuPt_B$ ordering rather than single-variant ordering due to the surface step geometry. We discuss how dual-variant ordering leads to a variable glide force, and thus has a different impact on dislocation dynamics than single-variant ordering. Because the III-V on Si nucleation procedure determines the step geometry, it also influences the dislocation dynamics.

ACCEPTED MANUSCRIPT

Pursuant to the DOE Public Access Plan, this document represents the authors' peer-reviewed, accepted manuscript. The published version of the article is available from the relevant publisher.

ACCEPTED MANUSCRIPT

1 Introduction

Compositionally graded buffers have successfully enabled many types of lattice-mismatched epitaxial devices such as lasers, transistors, light-emitting diodes, and multijunction solar cells [1-7]. The compositionally graded buffer transitions the lattice constant from the substrate's lattice to other useful lattice constants for the device, but introduces some undesirable material properties such as surface roughness, variable surface strain and composition, and threading dislocations [8-10]. For minority carrier devices such as III-V multijunction solar cells, a very low threading dislocation density, 10^6 cm^{-2} or lower, is needed to limit nonradiative recombination and achieve a high power conversion efficiency [11, 12].

GaAsP compositionally graded buffers on silicon substrates enable access to the lattice constants needed for low-cost III-V multijunction solar cells [13-15]. However, the III-V on Si nucleation procedure requires careful control in order to avoid formation of anti-phase boundaries [16]. Recently, antiphase-domain free growth of III-V on silicon substrates has been demonstrated by multiple labs by careful control of the GaP/Si nucleation procedure [17-21]. Then, using high quality APD-free III-V-on-Si templates, K.N. Yuang and M. Vaisman et al. [22, 23] showed that GaAsP compositionally graded buffers can transition the lattice constant from Si to $GaAs_{0.76}P_{0.24}$ while maintaining a threading dislocation density (TDD) of 4×10^6 cm^{-2}, potentially enabling high efficiency 2-junction solar cells if combined with a high-quality active silicon subcell [24]. Clear progress has been made towards III-V on Si epitaxial integration for multijunction cells. However, significant improvement in device performance is expected with further lowering the threading dislocation density. In addition, lowering the required buffer thickness will reduce cost as well as avoid cracking due to thermal expansion coefficient mismatch [25], which becomes both a performance concern and a reliability concern when the total III-V layer thickness is beyond a critical value.

The threading dislocation density of a compositionally graded buffer is lowest with facile dislocation glide and limited dislocation nucleation. Material properties of the graded buffer, such as composition fluctuations, surface morphology, internal defects, and atomic ordering, can have a large influence over dislocation nucleation and glide energies, and so must be investigated and controlled [26]. Internal material properties change throughout the buffer by necessity as the composition changes, requiring a material-based study throughout the expected composition range. First, material properties that limit glide or lead to enhanced dislocation nucleation must be identified. Then, the cause of any undesirable material properties can be studied and the buffer can be optimized by altering the structure and growth conditions.

In this paper, we perform an investigation into the material properties of GaAsP graded buffers between GaP and GaAs lattice constants on both GaP and Si substrates, with the intent of determining factors that influence the residual threading dislocation density. In the first section, we investigate atomic ordering and phase separation on GaP substrates using transmission electron microscopy (TEM) and X-ray diffraction (XRD). Phase separation is not observed, but single-

Pursuant to the DOE Public Access Plan, this document represents the authors' peer-reviewed, accepted manuscript. The published version of the article is available from the relevant publisher.

ACCEPTED MANUSCRIPT

variant $CuPt_B$ atomic ordering is present and has an impact on the dislocation glide plane distribution. In the next section, we analyze the TDD throughout sequential layers of the buffer using electron channeling contrast imaging (ECCI) in order to determine the impact of atomic ordering on the dislocation density, and measure the surface roughness throughout the buffer using atomic force microscopy. Finally, GaAsP buffers on Si substrates are investigated and observed to have dual-variant $CuPt_B$ ordering rather than single-variant ordering due to the substrate orientation and III-V on Si nucleation procedure. The influences of dual-variant $CuPt_B$ ordering on dislocation behavior are discussed.

2 Background

Phase separation and atomic ordering are well studied in III-V materials, and are known to impact dislocation glide [26, 27]. Phase separation in GaAsP has not been previously observed, and is not predicted by delta lattice parameter or regular solution miscibility calculations for bulk material [28, 29]. However, III-V phase separation often occurs at the epitaxial surface, leading to higher critical temperatures than bulk material calculations and thus the need for experimental observation [30, 31].

Stringfellow et al. observed atomic ordering of the group-V sublattice while studying single epilayers of GaAsP [32, 33]. Others have studied GaAsP graded buffers, but atomic ordering in GaAsP buffers has not been reported [34-36]. Atomic ordering impacts dislocation energetics in III-V materials, which has been investigated in lattice-mismatched compressive GaInP on GaAs substrates. A detailed description is included in previous publications [37-40], and a brief review is included here to aid interpretation of later results.

Atomic ordering has been well investigated in GaInP, and typically consists of alternating (111)B planes of GaP-rich and InP-rich material, termed $CuPt_B$ ordering. Figure 1 shows a generic III-V material with $CuPt_B$ atomic ordering, which is directly applicable to GaInP or GaAsP. In GaInP, the $CuPt_B$ ordered structure is grown into the alloy due to the surface reconstruction, which consists of long rows of phosphorus dimers [41], and is sensitive to all growth conditions, including growth rate, growth temperature, surfactants and dopants [42]. In addition, the substrate orientation influences the type and strength of ordering [43]. The step geometry of an (001) substrate miscut towards $(\bar{1}11)$B planes gives preference for $CuPt_B$ ordering of a single-variant, where ordering only exists in the $[\bar{1}11]$B direction. (001) substrates with a miscut towards (111)A planes have a different step geometry that does not lead to the same preference for a single ordering variant, and so dual-variant $CuPt_B$ ordering occurs, with domains of ordering along $[\bar{1}11]$B and $[1\bar{1}1]$B both present.

Pursuant to the DOE Public Access Plan, this document represents the authors' peer-reviewed, accepted manuscript. The published version of the article is available from the relevant publisher.

ACCEPTED MANUSCRIPT

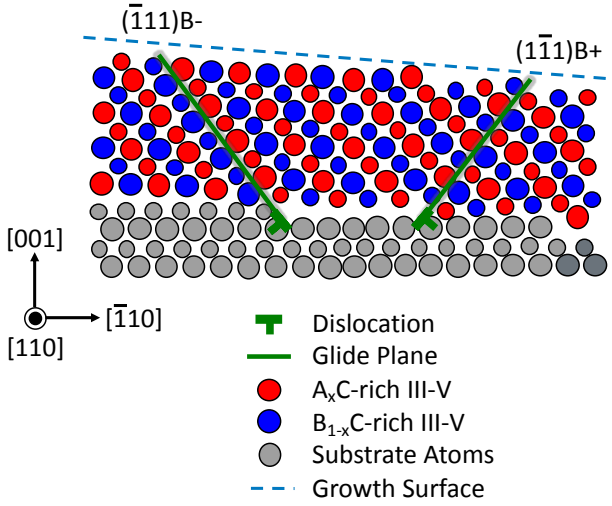

Fig. 1. Illustration of glide in single-variant $CuPt_B$-ordered $A_xB_{1-x}C$ or AC_yD_{1-y}, showing $A_xB_{1-x}C$ as an example. Single-variant ordering is encouraged by the (001) substrate miscut towards $(\bar{1}11)$B-, and has alternating $(\bar{1}11)$B- planes of A_xC-rich alloy and $B_{1-x}C$-rich alloy. Glide along $(1\bar{1}1)$B+ creates an energetically favorable anti-phase boundary in the order pattern, while glide along $(\bar{1}11)$B- does not.

In bulk III-V material, the ordered structure is metastable [44]. Annealing can disorder the material [45], although the ordered structure commonly persists throughout growth. Dislocation glide through ordered planes disrupts the order pattern and is energetically favorable in III-V compounds because glide reduces this metastability. Dislocation glide through ordered planes thus creates an anti-phase boundary in the order pattern, which should not be confused with anti-phase boundaries created in GaP upon GaP/Si nucleation. The release of additional energy via glide through ordered planes leads to a reduction in the critical thickness [39], and a skewing of the population of dislocations towards those that disrupt the order pattern [38]. With single-variant $CuPt_B$ ordering in the $[\bar{1}11]$ direction, dislocations with [011] and $[\bar{1}01]$ Burgers vectors disrupt the order pattern, which leads to a preference for glide on $(1\bar{1}1)$ planes for dislocations with [110] line direction. Figure 1 illustrates how glide along $(1\bar{1}1)$B+ involves an atomic shift that disrupts the order pattern, while glide along $(\bar{1}11)$B- does not disrupt the order pattern.

An imbalance of dislocation glide between $(1\bar{1}1)$B+ and $(\bar{1}11)$B- planes leads to a tilt in the epilayer with respect to the substrate that is measurable using X-ray diffraction [46, 47]. A tilt that reduces the angle between the substrate and (004) planes indicates dominant glide on the $(\bar{1}11)$B- plane, here also called the "B-" plane, and tilt that increases this angle indicates dominant glide on the $(1\bar{1}1)$B+ plane, here also called the "B+" plane, and shown in Figure 1. The percentage of dislocation glide occurring on one of these planes, P_{B+}, throughout the buffer can be quantified from the tilt, α_B, and the amount of relaxed strain, $\Delta\varepsilon_B$, using [38]:

$$P_{B+} = \frac{1}{2} + \frac{\tan \alpha_B}{2\sqrt{2}\Delta\varepsilon_B} \qquad \text{(Eq. 1)}$$

Pursuant to the DOE Public Access Plan, this document represents the authors' peer-reviewed, accepted manuscript. The published version of the article is available from the relevant publisher.

ACCEPTED MANUSCRIPT

where the tilt and relaxed strain are caused by dislocations on the B planes, and tilt is defined such that positive tilt increases the miscut angle.

Due to its metastability, atomic ordering presents an additional force acting upon dislocations. Glide forces are affected by the strength of the ordering, and can change upon order-disorder transitions. In previous work, a transition between dominant glide planes occurred upon an ordering-induced change in glide force in GaInP buffers, which was observed as a change in the net direction of tilt throughout a graded buffer [38]. During this transition, an increase in the threading dislocation density was also observed. Changes in tilt throughout a buffer imply changes to the driving forces for dislocation motion, and are thus worthy of investigating since the underlying cause may also drive dislocation formation.

3 Experimental Methods

III-V epitaxy was performed in a 7 x 4" AIXTRON Crius Close-Coupled Showerhead reactor using (001) GaP substrates miscut 2° towards (011) as well as GaP/Si templates. The GaP/Si templates were created in the same reactor but prior to the GaAsP growth using triethylgallium (TEGa) and tertiarybutylphosphine (TBP) precursors, and the general nucleation procedure described by Volz et al. [17]. Briefly, (001) silicon substrates miscut 2° toward (111) were first deoxidized at 950 °C in a hydrogen ambient at 950 mbar. Then, a double-stepped surface was created by slowly ramping the temperature from 1050 to 500 °C under hydrogen at a reactor pressure of 950 mbar. Initial monolayers of GaP were deposited at 100 mbar using migration enhanced epitaxy at 450 °C, after which 60 nm of GaP is deposited at 580 °C.

The GaP substrates oriented towards (001) with 2° miscut towards (011) along with the GaP/Si templates, where the Si is oriented towards (001) with 2° miscut towards (111) were co-loaded into the Crius reactor for GaAsP growth. GaAsP layers were grown at 100 mbar and at 700 °C surface temperature (measured via pyrometry) with a growth rate of 2.7 μm/h and a V/III ratio of 40 using triethylgallium (TEGa), arsine, and phosphine precursors with silane (SiH_4) as a silicon dopant source. Previously-grown calibration samples were used to determine the nonlinear mixed-anion incorporation.

Seven Si-doped GaAsP buffers of various thicknesses were grown on each type of substrate by ending the buffer after a different number of GaAsP layers. Each layer was nominally 250 nm thick and 0.25% mismatched to the previous layer, leading to a strain-grading rate of 1%/μm. Six of these Si-doped samples ended after 4, 6, 8, 10, and 12 layers, leading to buffers of nominally 1.0, 1.5, 2.0, 2.5, and 3.0 % total mismatch (wrt GaP) and 1.0, 1.5, 2.0, 2.5, and 3.0 μm total thickness. One final Si-doped GaAsP buffer was grown to the GaAs lattice constant with 14 layers, for a total thickness of 3.5 μm, with an additional 1 μm thick AlGaAs/GaAs/AlGaAs double-heterostructure (DH) cap layer for analysis. This structure was repeated using diethyltellurium (DETe) as a tellurium surfactant and dopant precursor rather than silane. Both Si and Te doping levels target nominally 1 x 10^{18} cm^{-3} carrier concentration throughout the buffer, determined separately.

Pursuant to the DOE Public Access Plan, this document represents the authors' peer-reviewed, accepted manuscript. The published version of the article is available from the relevant publisher.

ACCEPTED MANUSCRIPT

The threading dislocation density of the various buffers was determined using Electron Channeling Contrast Imaging (ECCI) in a Hitachi SU-70 SEM with a Schottky field emission gun at 30 kV acceleration voltage and a 4-quadrant back scattered electron (BSE) detector, measuring at least 50 dislocations for each sample in an area between 500 – 2000 μm^2. Atomic force microscopy (AFM) was performed in a Park tool in non-contact mode with the crosshatch roughness at 45° to the scanning direction, averaging an area of over 400 μm^2.
Transmission electron diffraction and dark-field transmission (DFTEM) was performed using a JEOL JEM-3010. Lift-out cross-section samples were prepared in both [110] and [$\bar{1}$10] using a JEOL JIB-4601F with a final gallium ion polishing at 1 kV, resulting in a thickness well below 150 nm. In addition, aberration-corrected scanning TEM was carried out using a JEOL JEM-2200FS in order to verify the GaP polarity and existence of phase ordering.

High resolution X-ray diffraction was performed on a Panalytical X'Pert Pro diffractometer. Atomic ordering was observed using ½(113) skew symmetric planes, and reciprocal space maps (RSMs) of (004) planes from both (110) and ($\bar{1}$ 10) incidence were used to monitor the lattice tilt throughout the buffer. RSMs from (224)GI (glancing incidence) planes were also used to determine the room-temperature strain and composition throughout the buffer.

4 Investigation of bulk material properties of GaAsP on GaP

A GaAsP graded buffer spanning the full ternary composition range from GaP to GaAs is grown on a (001) GaP substrate miscut 2° towards (011) at 700 °C and with a growth rate of 2.7 μm/h and a V/III ratio of 40. The (011) miscut bisects the (111)A and ($\bar{1}$11)B planes, and so the surface contains steps of both types. An illustration of the buffer structure is shown in Fig. 2(a). TEM and XRD are performed on this sample to study phase separation and ordering.

ACCEPTED MANUSCRIPT

Pursuant to the DOE Public Access Plan, this document represents the authors' peer-reviewed, accepted manuscript. The published version of the article is available from the relevant publisher.

ACCEPTED MANUSCRIPT

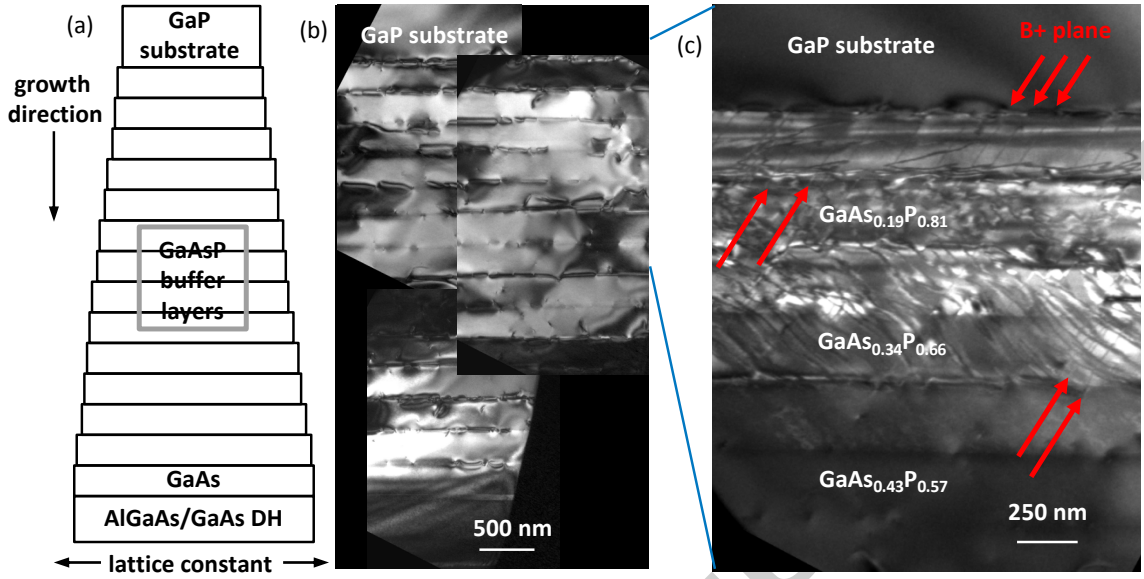

Fig 2. (a) Illustration of GaAsP buffer structure studied in section 4.1. The substrate is (001) GaP with a 2° miscut towards (011), and the buffer extends to the GaAs lattice constant. (b) Stitched 002 DF image from the [110] pole showing the entire GaAsP buffer, where the layers in the image correspond to the illustration. No phase separation is observed. (c) ½ 111 DF image from the [110] pole of the first several layers of the GaAsP buffer. The strength of the ordering throughout the buffer can be qualitatively determined from the intensity, and anti-phase boundaries in the order pattern are observed as either sharp contrast (from dislocation glide on B+ planes, highlighted) or wavy contrast (grown-in).

4.1 TEM and XRD results

Figure 2(b) shows a stitched DFTEM image from the chemically sensitive 002 diffraction of the entire GaAsP buffer, taken from the [110] pole. No contrast features indicative of composition fluctuations are observed, indicating a uniform composition within each layer and non-existent or very limited phase separation. The observed long-scale contrast features are from sample bending and thickness variation inevitable for large scale thin TEM foils from strained materials. During investigation suitable 002 DF tilt corrections were set for the images independently.

Transmission electron diffraction patterns from the first six layers of the buffer, shown in the insets of Fig. 3, show single-variant $CuPt_B$ ordering, identified by the existence of $(1\bar{1}1)$ superlattice spots. Single-variant ordering is also confirmed using XRD by the diffraction from one set of ½(113) skew symmetric planes (shown later in Figure 5). From XRD, the relationship between the surface miscut and the ordering planes can be identified: the ordered planes are in the same direction as the $(\bar{1}11)$B portion of the miscut, which is also found in GaInP [41] and as illustrated in Fig. 1.

Pursuant to the DOE Public Access Plan, this document represents the authors' peer-reviewed, accepted manuscript. The published version of the article is available from the relevant publisher.

ACCEPTED MANUSCRIPT

The TEM dark field imaging of the ½($\bar{1}$11) superlattice spot in Fig. 2(c) shows that the atomic ordering only exists for the first few layers of the buffer. The strength of the ordering throughout the buffer can be qualitatively gauged by the strength of the contrast in this diffraction condition. While the contrast increases in the first two GaAsP buffer layers, no contrast is observed after the 5th layer, indicating that ordering is not present or is very weak at compositions above $GaAs_{0.4}P_{0.6}$ (As content > 0.4). Contrast from anti-phase boundaries in the ordering is observed in Fig. 2(c), which have also been reported by other authors in superlattice DF imaging of GaInP [38, 48, 49]. The large wavy contrast features, mostly parallel to ($\bar{1}$11)B- planes, are due to grown-in anti-phase boundaries. The sharp contrast on (1$\bar{1}$1)B+ planes are from dislocations that glide through ordered planes, creating anti-phase boundaries in the order pattern along the slip plane, as illustrated in Fig. 1.

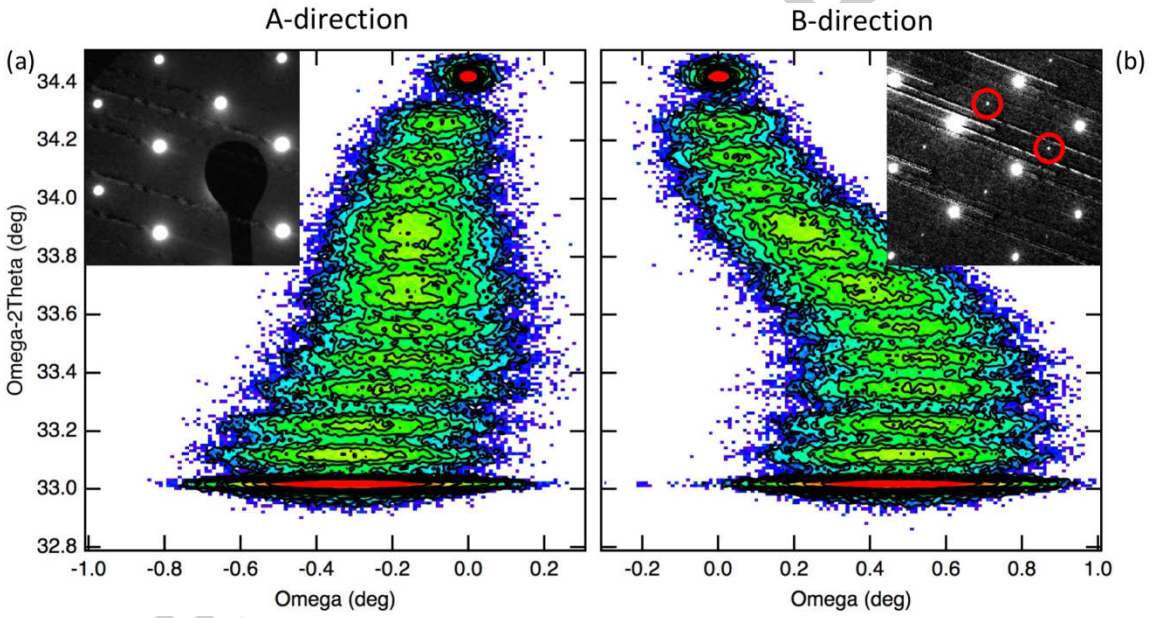

Fig. 3. High resolution X-ray diffraction reciprocal space maps of the GaAsP buffer, diffracted from (004) planes taken with the incident beam in the (a) ($\bar{1}$10) plane, testing strain and tilt in the A-direction, and (b) (110) plane, testing strain and tilt in the B-direction. The layers with different composition in the GaAsP buffer can be identified, and correspond to the illustration in Figure 2a. The Omega axis of these (004) scans is due to epilayer tilt around the measurement axis with respect to the substrate: (a) observes tilt around [$\bar{1}$10] and (b) observes tilt around [110]. The insets are the associated transmission electron diffraction patterns: (a) from the [$\bar{1}$10] pole and (b) from the [110] pole. The angled lines in the diffraction patterns are detector artifacts. Single-variant $CuPt_B$ ordering is observed from the [110] pole, indicated by superlattice spots (circled), as well as a net positive tilt, indicating glide through ordered planes.

The XRD RSM of (004) planes of the GaAsP buffer using X-rays incident in the ($\bar{1}$10) plane is shown in Fig. 3(a), and using (110) incidence in Fig. 3(b). We refer to [110] as the A-direction and [$\bar{1}$10] as the B-direction, which are tested with ($\bar{1}$10) and (110) incident X-rays, respectively. The Omega axis corresponds to the tilt with

Pursuant to the DOE Public Access Plan, this document represents the authors' peer-reviewed, accepted manuscript. The published version of the article is available from the relevant publisher.

ACCEPTED MANUSCRIPT

respect to the substrate around [$\bar{1}$10] in Fig. 3(a), and around [110] in Fig. 3(b). The epilayer tilt around both axes changes throughout the buffer. Tilt that reduces the angle between the growth plane of the miscut substrate and (004) planes is negative in the x-axis of Fig. 3, while tilt that increases this angle is positive.

The glide plane distribution throughout the buffer is determined from Eq. 1 by measuring the tilt, relaxed lattice constant, and residual strain of each layer using XRD RSMs of both (004) and (224)GI planes from both ($\bar{1}$10) and (110) incidences, which tests dislocations gliding on A planes and B planes, respectively. The amount of strain relaxed in layer x with respect to the previous layer, $\Delta\varepsilon_x$, is calculated from the difference between the residual strain of layer x, $\varepsilon_x = (a_{//,x} - a_{r,x})/a_{r,x}$, and the total misfit of layer x with respect to the in-plane lattice constant of the previous layer, $\Delta f_x = (a_{//,x-1} - a_{r,x})/a_{r,x}$, where $a_{r,x}$ is the relaxed lattice constant of layer x, $a_{//,x}$ is the in-plane lattice constant of layer x, and $a_{//,x-1}$ is the in-plane lattice constant of the layer prior to layer x. Thus, $\Delta\varepsilon_x = \Delta f_x - \varepsilon_x = (a_{//,x-1} - a_{//,x})/a_{r,x}$.

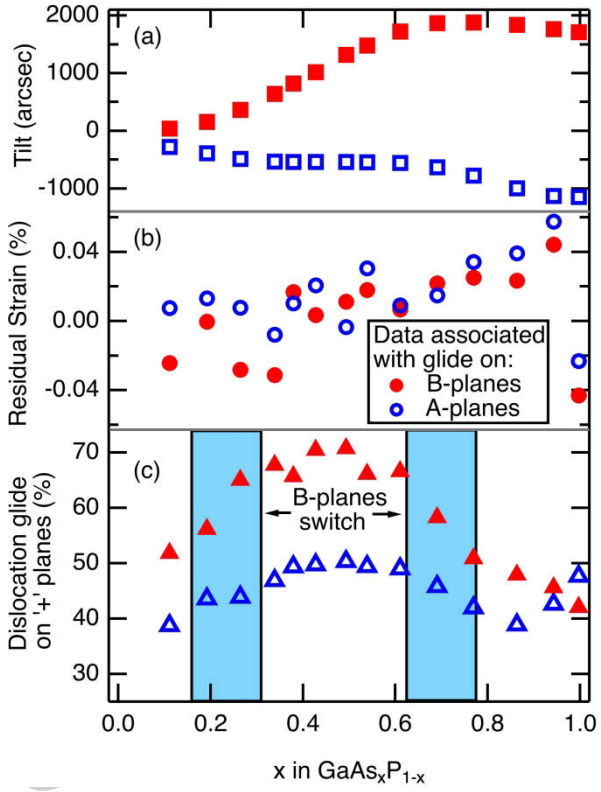

Fig. 4. (a) Epilayer tilt, (b) residual strain, and (c) glide plane distribution as a function of GaAsP composition, for all 14 layers of the GaAsP buffer on GaP. All results are calculated from XRD. Data corresponding to glide on B planes (dislocations with [110] line direction, and corresponding to XRD data measured using (110) incidence) is colored red, while data corresponding to glide on A planes (dislocations with [$\bar{1}$10] line direction and corresponding to XRD data using ($\bar{1}$10) incidence) is colored blue. The B-planes have two large switches in glide plane distribution, which are highlighted in (c).

Pursuant to the DOE Public Access Plan, this document represents the authors' peer-reviewed, accepted manuscript. The published version of the article is available from the relevant publisher.

ACCEPTED MANUSCRIPT

Figure 4 shows the room-temperature residual strain, tilt, and calculated percentage of glide on planes that result in positive tilt, as a function of the composition of the layer, which is determined from the relaxed lattice constants of the layer using Vegard's law [50]. Data is listed by the relevant parameters for dislocations with both [110] and [$\bar{1}$10] line directions in red and blue, respectively, which correspond to glide on B planes and A planes, respectively. The residual strain is low throughout the buffer, and becomes tensile near the end of the buffer, likely due to thermal expansion coefficient mismatch upon cooldown. The final layer has more compressive strain than the previous layers, as is typical in graded buffers [51]. The tilt and glide plane distribution change throughout the buffer, and are markedly different between the two sets of dislocations. Changes in the direction of tilt, and thus changes in the glide plane distribution, imply changes in the driving forces for dislocation glide throughout the buffer. In this case, the observed changes will be related to the type of atomic ordering and the substrate miscut, discussed in the next section.

4.2 Discussion

Phase separation in GaAsP has not been previously observed [34], and is not predicted by miscibility calculations for bulk material. No phase separation is observed by TEM imaging, ruling out phase separation as a limitation to dislocation glide.

$CuPt_B$ atomic ordering of the group-V sublattice is observed in the GaAsP graded buffer. Stringfellow et al. also observed $CuPt_B$ GaAsP atomic ordering of the group-V sublattice while studying single epilayers [32, 33]. Others have studied GaAsP graded buffers, but not observed atomic ordering [34-36]. Interestingly, GaAsP buffers have been previously shown to have anomalous tilt behavior consistent with the tilt observed in this study [52, 53], but ordering was not observed.

The atomic ordering in the GaAsP in Fig. 2 varies in strength throughout the graded buffer. Atomic ordering naturally varies with the composition of a ternary alloy. In this case of a GaAsP graded buffer on a GaP substrate, the maximum possible ordering initially increases with As-content towards the purely mixed ternary, $GaAs_{0.5}P_{0.5}$, where a perfectly ordered structure is possible. Thus, the observed increase in strength of the ordering in the first few layers of the buffer is expected. However, the TEM shows the strongest superlattice diffraction around layer 4, $GaAs_{0.34}P_{0.66}$, and that ordering is absent by layer 6, $GaAs_{0.43}P_{0.57}$. The decrease in strength of the ordering is not expected based on the composition, and differs from findings on single epilayers [33].

The reason for the decay in the strength of atomic ordering in these layers is not fully understood, but there may be multiple influences. Changes to the surface reconstruction as the As/P ratio changes throughout the buffer may influence the strength of the ordering by affecting the strength of surface dimerization. In a previous study, Jun et al. found that the strength of ordering in GaInP decreases as arsenic is added [54], which is consistent with our finding for GaAsP. A related possibility is that the surface simply roughens throughout the buffer growth, as is

Pursuant to the DOE Public Access Plan, this document represents the authors' peer-reviewed, accepted manuscript. The published version of the article is available from the relevant publisher.

ACCEPTED MANUSCRIPT

typical for compositionally graded buffers, and this roughness affects the surface reconstruction and ordering strength.

Annealing may also influence the strength of ordering throughout growth. Atomic ordering is not thermodynamically stable and has previously been shown to reduce upon annealing in GaInP [44, 45]. In this case, the ordered structure is grown into the GaAsP at the surface and then annealed during the subsequent layers of the growth. The temperature required to reduce the atomic ordering by annealing likely depends on the composition of the ternary, as does the melting point [55], and this composition dependence could lead to the observed decrease in the ordering at middle GaAsP layers the buffer despite the earlier layers of the buffer receiving a longer anneal. The influence of annealing has not been studied here, but could be performed by quantifying the order parameter of isolated GaAsP layers after various anneals.

Figure 4(c) shows that preferential glide on $(1\bar{1}1)$B+, presumably due to the presence of ordering, occurs until $GaAs_{0.7}P_{0.3}$, which is later in the buffer than the TEM shows ordering. The removal of ordering by annealing helps explain this discrepancy as well as the difference in compositional range of ordering between this study and those by Chen et al. [33]. We also note that previous studies have observed preferential glide on $(1\bar{1}1)$B+ in GaAsP and not reported ordering [52, 53, 56]. Subtle differences between growth conditions between this study and previous work may be related to the differences in results, and we also cannot rule out the possibility that something else is influencing glide, such as the surface.

The observed tilt in the GaAsP buffer in Fig. 3 is explainable by the known relationship between the substrate miscut and atomic ordering, and dislocation energetics, which has previously been described for GaInP graded buffers [38]. However, some important distinctions are present between GaAsP and the previous work on GaInP, described below.

The present GaAsP buffer is grown on an (001) GaP substrate with a small, 2°, miscut towards (011), which contains components of miscut towards (111)A and $(\bar{1}11)$B, and thus steps along both [110] and $[\bar{1}10]$ directions. The substrate miscut rotates the glide planes with respect to the in-plane strain, and leads to a preference for glide on "-" planes, $(\bar{1}11)$B- and (111)A-, for these substrates due to an increase in strain relief on "-" planes [57]. The substrate contains equivalent miscut components in both A- and B-directions but only the B-direction is influenced by ordering, which allows comparison of the influence of miscut alone (A-direction) with the influence of both the miscut and atomic ordering (B-direction) in these samples.

In the A-direction, the tilt is simply a result of the substrate miscut with no influence from ordering. The component of the substrate miscut towards (111)A affects dislocations with $[\bar{1}10]$ line directions (α-dislocations) by leading to a preference for (111)A- glide over $(\bar{1}\bar{1}1)$A+ glide, observed via XRD using $(\bar{1}10)$ incidence. Each glide plane for $[\bar{1}10]$ dislocations contains one Burgers vector that disrupts ordering, so there is no impact of ordering on the glide plane distribution. Thus, negative tilt is observed from $(\bar{1}10)$ incidence in Fig 3(a). A region in the middle of the buffer lacks tilt, which may indicate a glide limitation at this point.

Pursuant to the DOE Public Access Plan, this document represents the authors' peer-reviewed, accepted manuscript. The published version of the article is available from the relevant publisher.

ACCEPTED MANUSCRIPT

In the B-direction, both the substrate miscut and atomic ordering influence the tilt behavior. The component of the substrate miscut towards $(\bar{1}11)$B affects [110]-running dislocations (β-dislocations) by leading to a preference for $(\bar{1}11)$B- planes over $(1\bar{1}1)$B+ planes. The initial layers have a low As-content, and so the maximum possible order parameter is also low due to the composition. Thus, the influence of ordering (which favors glide on B+ planes) on glide plane distribution is low in these layers and balanced by the substrate miscut, which favors B- glide. However, as the ordering strength initially increases throughout the buffer, $(1\bar{1}1)$B+ planes become more energetically favorable than $(\bar{1}11)$B- planes. A switch between preferred glide planes occurs that leads to a change in the progression of tilt in the first layers of the buffer, as has been modeled previously [37]. Interestingly, positive tilt increases the effective miscut, which leads to additional driving forces on $(\bar{1}$ 11)B-. Later in the buffer, the strength of the atomic ordering decreases, leading to an additional glide plane switch from $(1\bar{1}1)$B+ to $(\bar{1}11)$B- in near $GaAs_{0.7}P_{0.3}$, which is observed in the XRD RSM in Fig. 3(b) as a change from positive-progressing tilt to negative-progressing tilt.

The observed glide plane switches are expected in compositionally graded buffers with variable single-variant ordering. They indicate changes in dislocation energetics throughout the buffer due to changes in the strength of ordering. However, glide plane switches have previously been correlated with an increased dislocation density in GaInP graded buffers [38], and so the impact of ordering on the threading dislocation density in GaAsP buffers must similarly be determined.

4.3 Control of ordering and glide plane distribution using Te surfactant

Surfactants such as Sb and Te are known to disrupt surface-driven atomic ordering in GaInP [58, 59]. To further test that the changes in glide plane distribution are related to ordering, a GaAsP buffer is grown on the same type of (001) GaP substrate miscut towards (011) with an identical structure and growth conditions to that in Figure 3, but with DETe flow instead of SiH_4 to provide a Tellurium surfactant in addition to a similar doping level, nominally 1×10^{18} cm^{-3}.

ACCEPTED MANUSCRIPT

Pursuant to the DOE Public Access Plan, this document represents the authors' peer-reviewed, accepted manuscript. The published version of the article is available from the relevant publisher.

ACCEPTED MANUSCRIPT

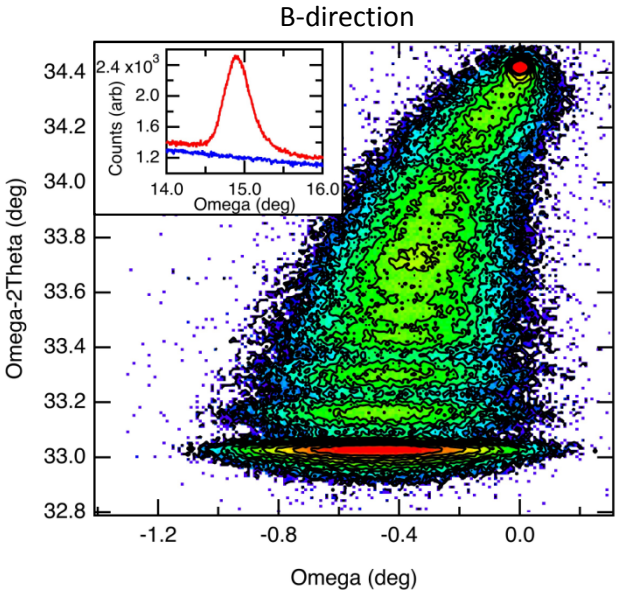

Fig. 5. XRD RSM of (004) planes, with the incident beam in the (110) plane (testing dislocations on B planes) of a GaAsP buffer identical to that in Figure 3, except for the replacement of Si doping with Te surfactant and doping. The direction of tilt is expected from the miscut, lacking influence from atomic ordering. (inset) XRD measurement of the ½(113) superlattice spot from the sample with Te surfactant (blue) and the sample in Figure 3 without Te surfactant (red), and no ordering is observed in the sample with Te surfactant.

Figure 5 shows the XRD RSM from 004 planes of the GaAsP on GaP buffer with Te surfactant, from (110) incidence, thus testing [110]-running dislocations gliding on B planes. The predominant progression of tilt is in the negative direction, implying dominant glide on $(\bar{1}11)$B- planes, and no glide plane switches are observed. This is consistent with the miscut providing the dominant force acting on dislocations.

Ordering is qualitatively determined by measuring the intensity of the ½ (113) skew symmetric spot using XRD. The inset of Fig. 5 shows the diffracted intensity from the superlattice spot associated with $CuPt_B$ ordering for the samples with (blue data) and without (red data) Te surfactant. The superlattice spot is present for the buffer grown without Te surfactant, but not for the buffer grown with Te surfactant. Thus, we conclude that Te surfactant removes ordering from GaAsP similar to its effect on GaInP, even though the ordering is on the group V sublattice for GaAsP rather than the group III sublattice like GaInP. The correlation between the negative tilt and lack of ordering strengthens the conclusion that $CuPt_B$ atomic ordering leads to positive tilt for GaAsP buffers. In addition, tellurium surfactant can be used to control atomic ordering as well as the glide plane distribution in GaAsP graded buffers, which highlights the importance of the growth surface and choice of dopant.

5 Threading dislocation density of GaAsP buffers on GaP

Pursuant to the DOE Public Access Plan, this document represents the authors' peer-reviewed, accepted manuscript. The published version of the article is available from the relevant publisher.

ACCEPTED MANUSCRIPT

A sequence of GaAsP graded buffers on miscut (001) GaP substrates are grown with nominally identical growth conditions and grade rate, but with varying final compositions. In this way, the progression of the threading dislocation density throughout the GaAsP can be measured using ECCI [60, 61], and the impact of ordering and its associated glide plane switches on the threading dislocation density can be determined.

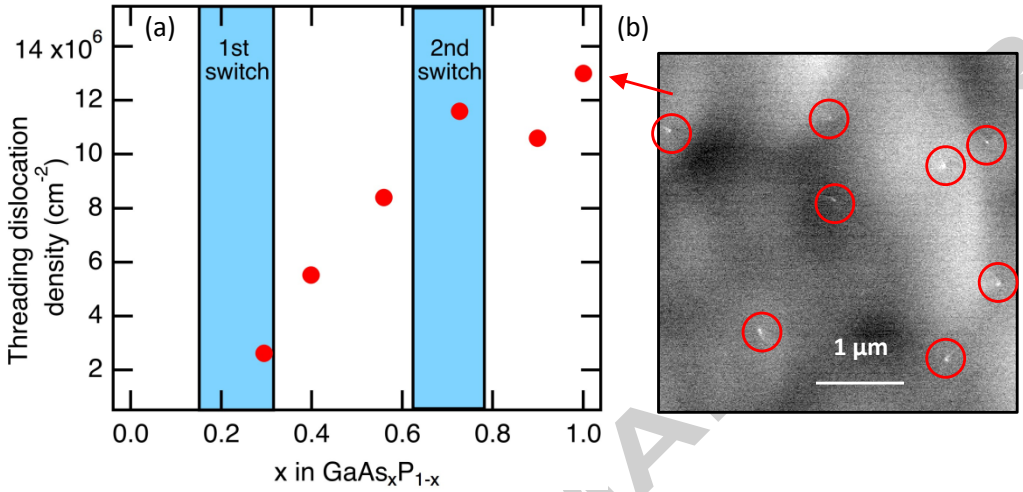

Fig. 6. (a) Threading dislocation density measured throughout the buffer in independent growths using ECCI. The blue regions correspond to glide plane switches determined from XRD, which are regions where the glide plane distribution is rapidly changing due to changes in dislocation energetics. (b) An example ECCI image from the buffer graded to the GaAs lattice constant. Red circles highlight individual threading dislocations.

Figure 6(a) shows the threading dislocation density throughout the GaAsP buffer, averaged over several scans totaling 500 – 2000 µm^2 area. Although the threading dislocation density at the composition $GaAs_{0.3}P_{0.7}$ is low, 2 x 10^6 cm^{-2}, the density then monotonically increases throughout the buffer and is 1.3 x 10^7 cm^{-2} at the GaAs lattice constant. The region in the buffer where glide plane switches occur are shown on the graph.

No clear increase in dislocation density occurs at the regions of the buffer where the dominant glide plane switches. This result differs from previous results for GaInP on GaAs substrates, where it was found that 100% of dislocations were gliding on $(1\bar{1}1)$B+ planes prior to the glide plane switch, and likely a very low density of dislocations with Burgers vectors on $(\bar{1}11)$B- planes existed. In our case, relaxation in the initial layers generates dislocations gliding on both planes, as is shown in the XRD results in Fig. 4(c). As glide energetics change due to changes in ordering, new dislocations do not need to form since they already exist on both planes.

The increase in TDD is then not related to phase separation or ordering-related glide plane distribution switches. This limits the TDD increase to either a naturally low dislocation velocity in GaAsP, or to a low activation energy for

Pursuant to the DOE Public Access Plan, this document represents the authors' peer-reviewed, accepted manuscript. The published version of the article is available from the relevant publisher.

ACCEPTED MANUSCRIPT

dislocation nucleation. While GaAsP has a lower glide velocity than III-V materials such as GaInAs or InAsP [62], the GaAsP glide velocity is expected to increase as the As-content increases, leading to a lower minimum required TDD throughout the buffer. Instead, the opposite trend is observed.

Previous GaAsP buffers grown by MBE displayed a high dislocation density with growth temperatures above 600 °C, which was explained by a low activation energy for nucleation [22]. Although GaAsP buffers grown by MBE may have different nucleation sources and activation energies, the results in this study can be similarly explained. Figure 7 shows the surface roughness throughout the buffer from the same sample set as Figure 6, and the insets show representative 20 x 20 μm AFM images from two samples with the z-scale set to 50 nm. We note that many factors lead to buffer surface roughening. However, the surface roughness slowly increases throughout the buffer along with the threading dislocation density, which is consistent with a surface-related dislocation nucleation source that has a low activation energy. Surface morphology is known to lead to dislocation nucleation [63].

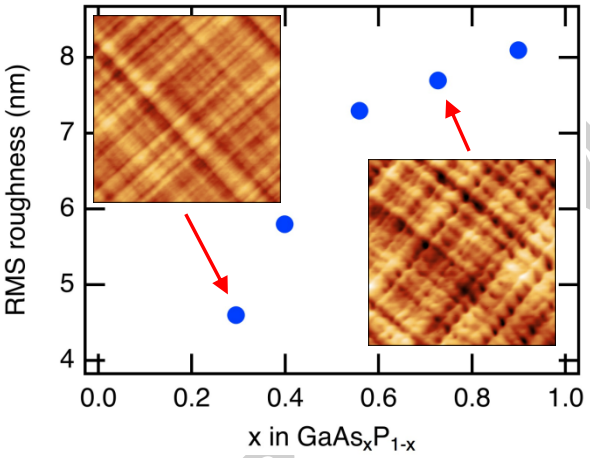

Fig. 7. AFM-measured RMS roughness throughout the buffer, using independent growths. The insets show two of the AFM images, both from a 20 x 20 μm area with the z-axis set to 50 nm.

Future efforts to reduce TDD should be placed on identifying the lowest energy dislocation nucleation source, and either eliminating it or avoiding it by altering growth conditions. Imaging the surface during the initial nucleation [64, 65] may determine whether dislocations nucleate at step edges, stress concentrators or other surface defects, and studying nucleation activation energies [22] may determine growth conditions to avoid excess nucleation, such as low growth temperature. Although the glide plane switches related to atomic ordering do not appear to play a role in the dislocation density, atomic ordering in GaInP has previously been shown to affect the surface morphology by creating facets [66], and so ordering may still be indirectly related to the TDD increase by introducing low energy dislocation nucleation sources on the surface, which requires a further systematic study.

Pursuant to the DOE Public Access Plan, this document represents the authors' peer-reviewed, accepted manuscript. The published version of the article is available from the relevant publisher.

ACCEPTED MANUSCRIPT

6 Dual-variant atomic ordering of GaAsP buffers on Si substrates

Anti-phase domain-free GaP/silicon templates were co-loaded into the reactor during all growths previously described. The dislocation density is markedly higher for the GaAsP buffers on GaP/silicon templates, as has also been observed previously [35]. After four GaAsP layers, at a composition of $GaAs_{0.3}P_{0.7}$, the dislocation density on the GaP/silicon templates is 1.5 x 10^7 cm^{-2}, whereas on GaP substrates it is 2 x 10^6 cm^{-2}. At the GaAs lattice constant, the dislocation density of the GaAsP buffer on GaP/Si is over 10^8 cm^{-2}, much higher than on GaP substrates. GaAsP buffers on GaP/Si templates have many differences from buffers on GaP substrates that may lead to a higher dislocation density. Here, we discuss differences in glide dynamics between these substrates related to ordering that play a role in the dislocation behavior and threading dislocation density, but are not necessarily the dominating reason for the threading dislocation disparity.

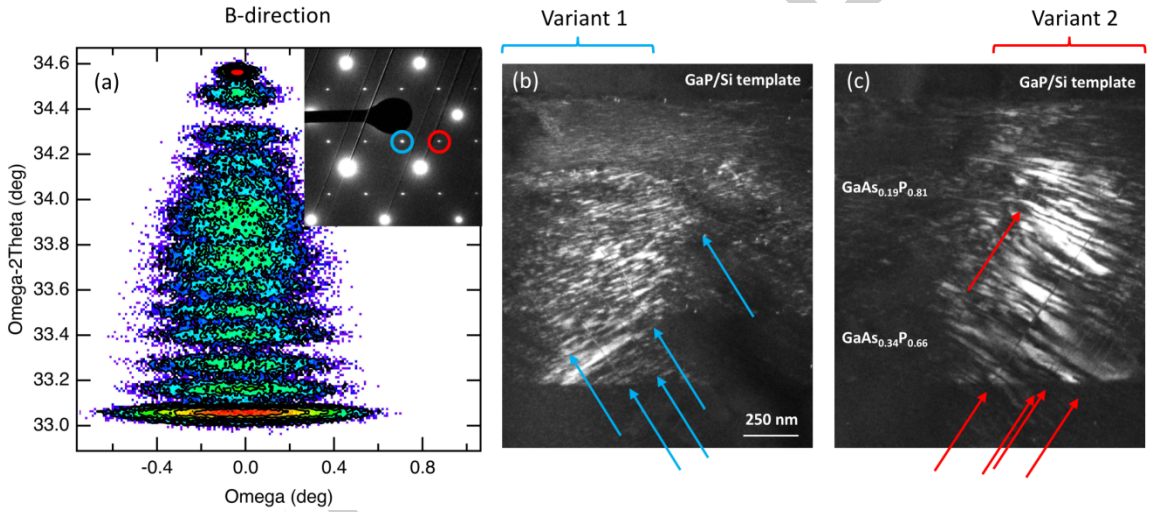

Fig. 8. (a) XRD RSM of (004) planes of the GaAsP buffer grown on GaP/Si templates. The incident beam is in the (110) plane, which tests dislocations gliding on B planes. The figure inset contains the corresponding diffraction pattern from the [110] pole, showing dual-variant $CuPt_B$ ordering. (b) and (c) show DF TEM imaging from the same location of the GaAsP buffer, performed using (b) ½($\bar{1}$11) and (c) the ½ (1$\bar{1}$1) superlattice spots. Different $CuPt_B$ variants (variant 1 and variant 2) are present in neighboring domains, and dislocations that disrupt the ordering are visible in either domain.

The GaAsP buffers on GaP/silicon templates have dual-variant $CuPt_B$ ordering, shown in the [110] cross-section transmission electron diffraction pattern in Fig. 8(a), rather than single-variant ordering observed on GaP substrates. The substrate orientation and type of GaP/Si nucleation influence the type of ordering in III-V. Here, the silicon substrates have (001) surfaces with a 2° miscut towards (111), as is typically used to encourage double-step formation and induce anti-phase domain-free growth. The type of GaP/Si nucleation procedure determines the polarity of the GaP, and the resulting surface step geometry. The GaP/Si nucleation used in this study leads to A-type steps on the GaP surface, as described previously [67]. III-V materials grown on (001) surfaces with either no miscut or purely A-type

Pursuant to the DOE Public Access Plan, this document represents the authors' peer-reviewed, accepted manuscript. The published version of the article is available from the relevant publisher.

ACCEPTED MANUSCRIPT

steps commonly display dual-variant $CuPt_B$ ordering, which is consistent with the observations of GaAsP buffers in this study. Dual-variant ordered III-V material contains domains of two variants of B-type ordering: some small domains of the material are ordered along $[1\bar{1}1]$ while other domains are ordered along $[\bar{1}11]$, illustrated in Fig. 9.

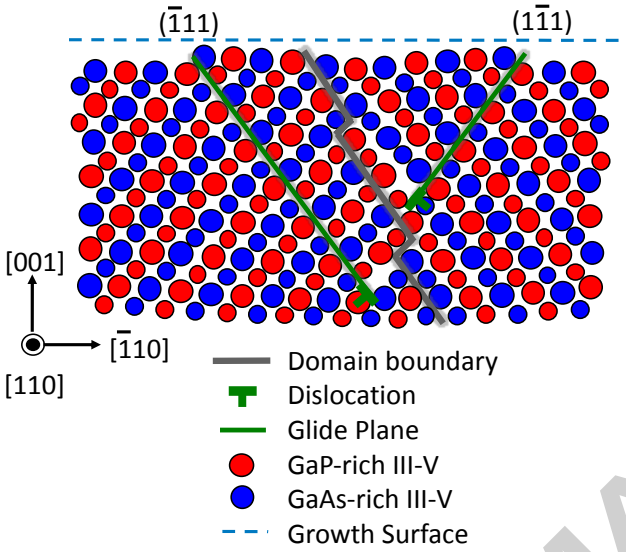

Fig. 9. Illustration of dislocation glide in GaAsP with dual-variant $CuPt_B$ ordering. Both $CuPt_B$ variants are shown in neighboring domains to highlight the influence of dual-variant ordering on dislocation behavior.

No tilt is observed in the XRD RSM of (004) planes from (110) incidence, testing B planes, shown in Figure 8(a), and none is expected. The miscut towards (111)A does not lead to an asymmetry in this direction. The ordered planes only lead to a glide plane preference within a local domain. Since equal strength of both domains is observed in the diffraction pattern, an equal distribution of dislocations gliding on $(\bar{1}11)$ and $(1\bar{1}1)$ is expected over a large area, resulting in no net tilt.

Figures 8(b) and 8(c) show dark-field TEM images of the superlattice spots, taken using the ½ $(\bar{1}11)$ diffraction and ½ $(1\bar{1}1)$ diffraction spots, respectively, both from the $[1\bar{1}0]$ cross-section, and both from exactly the same physical location of the buffer. Contrast is observed in the superlattice spots only in the first few layers of the GaAsP buffer on GaP/Si, similar to growth on GaP substrates, indicating that ordering exists only in the first few layers of the GaAsP buffer and is very weak or not present at compositions above $GaAs_{0.4}P_{0.6}$. DF imaging from one superlattice spot gives contrast for one ordering variant only. By imaging both superlattice spots independently, neighboring domains with opposing variants can be observed. APBs created from dislocation glide through ordered planes are visible within each variant as lines of sharp contrast, and are on opposing B-type glide planes in either variant. Thus, both sets of dislocations are generated and utilized to relieve strain, even in neighboring domains.

Pursuant to the DOE Public Access Plan, this document represents the authors' peer-reviewed, accepted manuscript. The published version of the article is available from the relevant publisher.

ACCEPTED MANUSCRIPT

Glide through ordered planes in GaAsP is energetically favorable. On GaP substrates, this leads to a positive tilt in the XRD RSM because the ordering is limited to a single-variant. On GaP/Si substrates, dual-variant ordering exists, where neighboring small domains contain one ordering variant or the other. Domains with different ordering variants enhance glide from dislocations with different Burgers vectors, illustrated in Fig. 9. Thus, throughout a dual-variant ordered material, a variable glide force exists for any given dislocation. Glide through a material with a variable glide force is not as efficient as through a material with a constant glide force, and has a similar effect on glide dynamics to composition fluctuations which are often observed in III-V materials [68-70]. A dislocation gliding in a domain with $CuPt_B$ variant 1 may stop gliding upon entering a domain with the $CuPt_B$ variant 2 due to an insufficient driving force. In addition, each domain has a driving force to nucleate dislocations that are locally favorable, potentially leading to higher nucleation rates in dual-variant material than single-variant material.

Differences in ordering between GaAsP buffers on Si and on GaP may play a role in the threading dislocation difference between the buffers, because dual-variant ordering inhibits efficient glide compared to single-variant material and may lead to enhanced nucleation. Dual-variant ordering introduces a variable glide force into the material, and so single-variant ordering is preferable. However, a more detailed analysis is necessary to determine the exact impact of dual-variant ordering on GaAsP graded buffers. In this study, both the type of substrate and the type of ordering change, which confounds an exact comparison of threading dislocation density.

7 Summary

GaAsP compositionally graded buffers grown on both GaP and Si substrates have been studied by XRD, TEM, ECCI, and AFM to identify potential limitations to dislocation glide. A detailed investigation is performed on GaAsP buffers grown at 700 °C with a growth rate of 2.7 μm/h and a V/III ratio of 40. Phase separation is not observed, but atomic ordering is observed and its impact on threading dislocation density is investigated.

On (001) GaP substrates with 2° miscut towards (011), GaAsP buffers display single-variant $CuPt_B$ atomic ordering. Ordering is only observed in layers with low As-content, and so the ordering has an unexpected composition dependence. Similar to ordered GaInP, glide through ordered GaAsP planes relieves internal energy in excess of the misfit strain energy, leading to a preference for glide on B+ planes when the order parameter is sufficiently high. The variation in order parameter throughout the buffer, combined with the natural preference for glide on B- planes due to the substrate miscut, leads to two switches in the dominant glide plane in GaAsP buffers that span the full ternary range from GaP to GaAs. Atomic ordering, and thus dislocation energetics and glide plane switches, can be controlled using tellurium surfactant. Thus, the surface plays a role in GaAsP buffer energetics as well as the choice of dopant.

The glide plane switches in the GaAsP buffers in this study do not drastically change the threading dislocation density, as measured in independent buffers

Pursuant to the DOE Public Access Plan, this document represents the authors' peer-reviewed, accepted manuscript. The published version of the article is available from the relevant publisher.

ACCEPTED MANUSCRIPT

ending with various compositions of GaAsP using ECCI. Instead, the threading dislocation density monotonically increases from 2 x 10^6 cm^{-2} to 1 x 10^7 cm^{-2} throughout the buffer independent of the glide-plane switches. Without internal glide limitations, the increase in dislocation density is likely due to a low activation energy for dislocation nucleation, which is consistent with the observed increase in surface roughness.

On (001) Si substrates with 2° miscut towards (111) and a thin GaP nucleation layer, GaAsP buffers display dual-variant $CuPt_B$ atomic ordering, and have a significantly higher threading dislocation density. Dual-variant ordering occurs because the GaP/Si nucleation procedure leads to A-type surface steps, which commonly leads to dual-variant ordering in III-V materials. Superlattice DF TEM imaging shows that neighboring domains with opposing $CuPt_B$ variants have dislocations gliding on opposing {111} glide planes.

Dual-variant ordering leads to a variable strain field for a given dislocation because each variant enhances glide from dislocations with different Burgers vectors. We theorize that glide is thus less efficient in dual-variant ordered material compared to single-variant ordered material, which may partially explain the increased dislocation density observed in GaAsP buffers on GaP/Si templates compared to GaP substrates.

In summary, we show that $CuPt_B$ atomic ordering can exist in GaAsP graded buffers on GaP and Si substrates and has an impact on dislocation energetics. With ordering present in GaAsP buffers, the type of miscut, GaP/Si nucleation procedure, and any growth conditions that influence the strength of the ordering, are important considerations in the design of GaAsP graded buffers because they indirectly affect dislocation behavior. Whether ordering influences the threading dislocation density will depend on how the relative energetics of ordering compare to the energetics of other factors affecting dislocations, such as dislocation nucleation energies and other influences on glide.

Acknowledgements

The authors would like to thank B. McMahon and K. Schulte for valuable conversations and S. Stättner for technical support. M. Feifel acknowledges the scholarship support from the German Federal Environmental Foundation (DBU). A. Beyer, K. Volz and J. Belz acknowledge support from the German Science Foundation (SFB 1083: “Structure and Dynamics of Internal Interfaces”). The work was supported in part by the German Federal Ministry of Education and Research through the project “MehrSi 03SF0525C” and in part by the U.S. Department of Energy under Contract No. DE-AC36-08GO28308 with Alliance for Sustainable Energy, LLC, the Manager and Operator of the National Renewable Energy Laboratory, with funding provided by the U.S. Department of Energy Office of Energy Efficiency and Renewable Energy Solar Energy Technologies Office. In 2012, the Global Alliance of Solar Energy Research Institutes (GA-SERI) was formed to strengthen institutional ties between NREL (U.S), Fraunhofer-ISE (Germany) and AIST (Japan). One key aspect to this alliance is a Researcher Exchange Program,

Pursuant to the DOE Public Access Plan, this document represents the authors' peer-reviewed, accepted manuscript. The published version of the article is available from the relevant publisher.

ACCEPTED MANUSCRIPT

which facilitated the sharing of techniques and information and led to the collaborative research described in this manuscript.

References

[1] D. Jung, L. Yu, S. Dev, D. Wasserman, M.L. Lee, Room-temperature mid-infrared quantum well lasers on multi-functional metamorphic buffers, Appl. Phys. Lett., 109 (2016) 211101.
[2] Y.-C. Xin, L.G. Vaughn, L.R. Dawson, A. Stintz, Y. Lin, L.F. Lester, D.L. Huffaker, InAs quantum-dot GaAs-based lasers grown on AlGaAsSb metamorphic buffers, J. Appl. Phys., 94 (2003) 2133.
[3] M.L. Lee, E.A. Fitzgerald, Strained Si, SiGe, and Ge channels for high-mobility metal-oxide-semiconductor field-effect transistors, J. Appl. Phys., 97 (2005) 011101.
[4] T.M. Christian, D.A. Beaton, K. Mukherjee, K. Alberi, E.A. Fitzgerald, A. Mascarenhas, Amber-green light-emitting diodes using order-disorder $Al_xIn_{1-x}P$ heterostructures, J. Appl. Phys., 114 (2013) 074505.
[5] F. Dimroth, R. Beckert, M. Meusel, U. Schubert, A.W. Bett, Metamorphic $Ga_yIn_{1-y}P/Ga_{1-x}In_xAs$ tandem solar cells for space and for terrestrial concentrator applications at C > 1000 suns, Prog. Photovolt., 9 (2001) 165.
[6] R.M. France, J.F. Geisz, I. Garcia, M.A. Steiner, W.E. McMahon, D.J. Friedman, T.E. Moriarty, C. Osterwald, J.S. Ward, A. Duda, M. Young, W.J. Olavarria, Design Flexibility of Ultra-High Efficiency Four-Junction Inverted Metamorphic Solar Cells, J. Photovolt., 6 (2016) 578.
[7] T.J. Grassman, D.J. Chmielewski, S.D. Carnevale, J.A. Carlin, S.A. Ringel, $GaAs_{0.75}P_{0.25}$/Si Dual-Junction Solar Cells Grown by MBE and MOCVD, J. Photovolt., 6 (2016) 326.
[8] E.A. Fitzgerald, Dislocations in Strained-Layer Epitaxy - Theory, Experiment, and Applications, Mater Sci Rep, 7 (1991) 91.
[9] R. Beanland, D.J. Dunstan, P.J. Goodhew, Plastic relaxation and relaxed buffer layers for semiconductor epitaxy, Advances in Physics, 45 (1996) 87.
[10] B.W. Dodson, J.Y. Tsao, Structural Relaxation in Metastable Strained-Layer Semiconductors, Annu. Rev. Mater. Sci., 19 (1989) 419.
[11] M. Yamaguchi, C. Amano, Efficiency calculations of thin-film GaAs solar cells on Si substrates, J. Appl. Phys., 58 (1985) 3601.
[12] C.L. Andre, D.M. Wilt, A.J. Pitera, M.L. Lee, E.A. Fitzgerald, S.A. Ringel, Impact of dislocation densities on n+/p and p+/n junction GaAs diodes and solar cells on SiGe virtual substrates, Journal of Applied Physics, 98 (2005) 014502.
[13] N. Jain, M.K. Hudait, III-V Multijunction Solar Cell Integration with Silicon: Present Status, Challenges, and Future Outlook, Energy Harvesting and Systems, 1 (2014) 121.
[14] J.F. Geisz, J.M. Olson, M.J. Romero, C.S. Jiang, A.G. Norman, Lattice-Mismatched GaAsP Solar Cells Grown on Silicon by OMVPE, 4th World Conf. on Photovoltaic Energy Conversion, IEEE, Hawaii, 2006.

ACCEPTED MANUSCRIPT

Pursuant to the DOE Public Access Plan, this document represents the authors' peer-reviewed, accepted manuscript. The published version of the article is available from the relevant publisher.

ACCEPTED MANUSCRIPT

[15] S.A. Ringel, T.J. Grassman, in: T. Li (Ed.) III-V Compound Semiconductors: Integration with Silicon-Based Microelectronics, CRC Press, Boca Raton, FL, 2011, pp. 523-576.
[16] H. Kroemer, Polar-On-Nonpolar Epitaxy, J. Crystal Growth, 81 (1987) 193.
[17] K. Volz, A. Beyer, W. Witte, J. Ohlmann, I. Németh, B. Kunert, W. Stolz, GaP-nucleation on exact Si(001) substrates for III/V device integration, J. Cryst. Growth, 315 (2011) 37.
[18] B. Kunert, I. Németh, S. Reinhard, K. Volz, W. Stolz, Si (001) surface preparation for the antiphase domain free heteroepitaxial growth of GaP on Si substrate, Thin Solid Films, 517 (2008) 140.
[19] T.J. Grassman, M.R. Brenner, S. Rajagopalan, R.R. Unocic, R.R. Dehoff, M. Mills, H. Fraser, S.A. Ringel, Control and elimination of nucleation-related defects in GaP/Si(001) heteroepitaxy, Appl. Phys. Lett., 94 (2009), 232106.
[20] E.L. Warren, A.E. Kibbler, R.M. France, A.G. Norman, P. Stradins, W.E. McMahon, Growth of antiphase-domain-free GaP on Si substrates by metalorganic chemical vapor deposition using an *in situ* AsH_3 surface preparation, Appl. Phys. Lett., 107 (2015), 082109.
[21] H. Döscher, T. Hannappel, B. Kunert, A. Beyer, K. Volz, W. Stoltz, *In situ* verification of single-domain III-V on Si(100) growth via metal-organic vapor phase epitaxy, Appl. Phys. Lett., 93 (2008) 172110.
[22] K.N. Yaung, M. Vaisman, J. Lang, M.L. Lee, GaAsP solar cells on GaP/Si with low threading dislocation density, Appl. Phys. Lett., 109 (2016) 032107.
[23] M. Vaisman, S. Fan, K.N. Yaung, E. Perl, D. Martin-Martin, Z.J. Yu, M. Leilaeioun, Z.C. Holman, M.L. Lee, 15.3%-Efficient GaAsP Solar Cells on GaP/Si Templates, ACS Energy Lett., 2 (2017) 1811.
[24] M. Feifel, T. Rachow, J. Benick, J. Ohlmann, S. Janz, M. Hermle, F. Dimroth, D. Lackner, Gallium Phosphide Window Layer for Silicon Solar Cells, J. Photovolt., 6 (2015) 384.
[25] V.K. Yang, M. Groenert, C.W. Leitz, A.J. Pitera, M.T. Currie, E.A. Fitzgerald, Crack formation in GaAs heteroepitaxial films on Si and SiGe virtual substrates, J. Appl. Phys., 93 (2003) 3859.
[26] R.M. France, F. Dimroth, T.J. Grassman, R.R. King, Metamorphic Epitaxy for Multijunction Solar Cells, MRS Bulletin, 41 (2016) 202.
[27] G.B. Stringfellow, G.S. Chen, Atomic Ordering in III/V Semiconductor Alloys, J. Vac. Sci. Technol. B, 9 (1991) 2182.
[28] G.B. Stringfellow, Miscibility gaps in quaternary III/V alloys, J. Cryst. Growth, 58 (1982) 194.
[29] K. Onabe, Calculation of Miscibility Gap in Quaternary InGaPAs with Strictly Regular Solution Approximation, Jap. J. Appl. Phys., 21 (1982) 797.
[30] S. Mahajan, Two-dimensional phase separation and surface-reconstruction driven atomic ordering in mixed III-V layers, Mater. Sci. Eng. B, 30 (1995) 187.
[31] I.P. Ipatova, V.G. Malyshkin, A.A. Maradudin, V.A. Shchukin, R.F. Wallis, Kinetic instability of semiconductor growth, Phys. Rev. B, 57 (1998) 12968.
[32] G.S. Chen, G.B. Stringfellow, Use of Surface Grooves to Control Ordering in GaAsP, Appl. Phys. Lett., 59 (1991) 3258.

Pursuant to the DOE Public Access Plan, this document represents the authors' peer-reviewed, accepted manuscript. The published version of the article is available from the relevant publisher.

ACCEPTED MANUSCRIPT

[33] G.S. Chen, D.H. Jaw, G.B. Stringfellow, Atomic Ordering in GaAsP, J. Appl. Phys., 69 (1991) 4263.
[34] M.J. Mori, S.T. Boles, E.A. Fitzgerald, Comparison of compressive and tensile relaxed composition-graded GaAsP and (Al)InGaP substrates, J. Vac. Sci. Technol. A, 28 (2010).
[35] J.R. Lang, J. Faucher, S. Tomasulo, K.N. Yaung, M.L. Lee, Comparison of GaAsP solar cells on GaP and GaP/Si, Appl. Phys. Lett., 103 (2013) 092102.
[36] T.J. Grassman, B. M.R., M. Gonzalez, A.M. Carlin, R.R. Unocic, R.R. Dehoff, M.J. Mills, S.A. Ringel, Characterization of Metamorphic GaAsP/Si Materials and Devices for Photovoltaic Applications, IEEE Trans. Electron Electron Devices, 57 (2010) 3361.
[37] W.E. McMahon, J. Kang, R.M. France, A.G. Norman, D.J. Friedman, S.-H. Wei, Ordering-enhanced dislocation glide in III-V alloys, J. Appl. Phys., 114 (2013) 203506.
[38] R.M. France, W.E. McMahon, A.G. Norman, J.F. Geisz, M.J. Romero, Control of misfit dislocation glide plane distribution during strain relaxation of CuPt-ordered GaInAs and GaInP, J. Appl. Phys., 112 (2012) 023520.
[39] R.M. France, W.E. McMahon, H.L. Guthrey, Critical Thickness of Atomically Ordered III-V Alloys, Appl. Phys. Lett., 107 (2015) 151903.
[40] A.G. Norman, R.M. France, W.E. McMahon, J.F. Geisz, M.J. Romero, The influence of atomic ordering on strain relaxation during the growth of metamorphic solar cells, J. Phys.: Conf. Series, 471 (2013) 012006.
[41] I.G. Batyrev, W.E. McMahon, S.B. Zhang, J.M. Olson, S.-H. Wei, Step structures on III-V phosphide (001) surfaces: How do steps and Sb affect CuPt ordering of $GaInP_2$?, Phys Rev Lett, 94 (2005) 096101.
[42] A. Mascarenhas, ed., Spontaneous ordering in Semiconductor Alloys, Kluwer Academic/Plenum Publishers, 2002.
[43] T. Suzuki, A. Gomyo, Sublattice ordering in GaInP and AlGaInP: effects of substrate orientations, J. Cryst. Growth, 99 (1990) 60.
[44] J.E. Bernard, R.G. Dandrea, L.G. Ferreira, S. Froyen, S.H. Wei, A. Zunger, Ordering in semiconductor alloys, Applied Physics Letters, 56 (1990) 731-733.
[45] P. Gavrilovic, F.P. Dabkowski, K. Meehan, J.E. Williams, W. Stutius, K.C. Hsieh, N. Holonyak, M.A. Shahid, S. Mahajan, Disordering of the ordered structure in MOCVD-grown GaInP and AlGaInP by impurity diffusion and thermal annealing, J. Cryst. Growth, 93 (1988) 426.
[46] J.E. Ayers, S.K. Ghandhi, L.J. Schowalter, Crystallographic Tilting of Heteroepitaxial Layers, J. Cryst. Growth, 113 (1991) 430.
[47] F.K. LeGoues, P.M. Mooney, J.O. Chu, Crystallographic tilting resulting from nucleation limited relaxation, Appl. Phys. Lett., 62 (1993) 140.
[48] C.S. Baxter, W.M. Stobbs, C.J. Gibbings, Observation of the Track of a Misfit Dislocation in Ordered $Ga_{0.5}In_{0.5}P$, Phil. Mag. Lett., 67 (1993) 59.
[49] E. Spiecker, M. Seibt, W. Schröter, R. Winterhoff, F. Scholz, Exploiting long-range atomic ordering for the investigation of strain relaxation in lattice-mismatched epitaxy: A case study on $CuPt_B$-type ordered (GaIn)P on GaAs, Applied Surface Science, 188 (2002) 61.

ACCEPTED MANUSCRIPT

Pursuant to the DOE Public Access Plan, this document represents the authors' peer-reviewed, accepted manuscript. The published version of the article is available from the relevant publisher.

ACCEPTED MANUSCRIPT

[50] S. Adachi, Properties of Semiconductor Alloys: group-IV, III-V, and II-VI, John Wiley and Sons Ltd, United Kingdom, 2009.
[51] S.P. Ahrenkiel, M.W. Wanlass, J.J. Carapella, R.K. Ahrenkiel, S.W. Johnston, L.M. Gedvilas, Optimization of buffer layers for lattice-mismatched epitaxy of $Ga_xIn_{1-x}As/InAs_yP_{1-y}$ double-heterostructures on InP, Solar Energy Materials and Solar Cells, 91 (2007) 908.
[52] T.J. Grassman, A.M. Carlin, K. Swaminathan, C. Ratcliff, J. Grandal, L. Yang, M.J. Mills, S.A. Ringel, Expanding the Palette: Metamorphic Strategies over Multiple Lattice Constant Ranges for Extendind the Spectrum of Accessible Photovoltaic Materials, Proceedings of the 37th IEEE PVSC, (2011) 003375.
[53] J. Ohlmann, Herstellung und Charakterisierung von metamorphen Pufferschichten für Ga(AsP)-Tandem-Solarzellen auf Si, Thesis, Philips-Universität Marburg, 2012.
[54] S.W. Jun, G.B. Stringfellow, J.K. Shurtleff, R.T. Lee, Isoelectronic surfactant-induced surface step structure and correlation with ordering in GaInP, J. Cryst. Growth, 235 (2002) 15.
[55] G.B. Stringfellow, Calculation of ternary phase diagrams, J. Phys. Chem. Solids, 33 (1972) 665.
[56] J. Schlies, Dislocation Distribution and Ordering in Metamorphic III-V Materials, Thesis, UCLA, 2014.
[57] F. Riesz, Crystallographic tilting in lattice-mismatched heteroepitaxy: A Dodson-Tsao relaxation approach, J. Appl. Phys., 79 (1996) 4111.
[58] J.K. Shurtleff, R.T. Lee, C.M. Fetzer, G.B. Stringfellow, Band-gap control of GaInP using Sb as a surfactant, Appl. Phys. Lett., 75 (1999) 1914.
[59] G.B. Stringfellow, R.T. Lee, C.M. Fetzer, J.K. Shurtleff, Y. Hsu, S.W. Jun, S. Lee, T.Y. Seong, Surfactant effects of dopants on ordering in GaInP, J. Electron. Mater., 29 (2000) 134.
[60] S. Zaefferer, N.-N. Elhami, Theory and application of electron channelling contrast imaging under controlled diffraction conditions, Acta Materialia, 75 (2014) 20.
[61] S.D. Carnevale et al., Applications of Electron Channeling Contrast Imaging for the Rapid Characterization of Extended Defects in III-V/Si Heterostructures, IEEE J. Photovolt., 5 (2015) 676.
[62] I. Yonenaga, Hardness, Yield Strength, and Dislocation Velocity in Elemental and Compound Semiconductors, Materials Transactions, 46 (2005) 1979.
[63] A.G. Cullis, A.J. Pidduck, M.T. Emeny, Growth morphology evolution and dislocation introduction in the InGaAs/GaAs heteroepitaxial system, J. Cryst. Growth, 158 (1996) 15.
[64] A.G. Cullis, A.J. Pidduck, M.T. Emeny, Misfit Dislocation Sources at Surface Ripple Troughs in Continuous Heteroepitaxial Layers, Phys. Rev. Lett., 75 (1995) 2368.
[65] D.E. Jesson, S.J. Pennycook, J.-M. Baribeau, D.C. Houghton, Direct Imaging of Surface Cusp Evolution During Strained-Layer Epitaxy and Implications for Strain Relaxation, Phys. Rev. Lett., 71 (1993) 1744.
[66] D.J. Friedman, J.G. Zhu, A.E. Kibbler, J.M. Olson, J. Moreland, Surface Topography and Ordering-Variant Segregation in $GaInP_2$, Appl. Phys. Lett., 63 (1993) 1774.

ACCEPTED MANUSCRIPT

Pursuant to the DOE Public Access Plan, this document represents the authors' peer-reviewed, accepted manuscript. The published version of the article is available from the relevant publisher.

ACCEPTED MANUSCRIPT

[67] O. Supplie, S. Brückner, O. Romanyuk, H. Döscher, C. Höhn, M.M. May, P. Kleinschmidt, F. Grosse, T. Hannappel, Atomic scale analysis of the GaP/Si(100) heterointerface by *in situ* reflection anisotropy spectroscopy and ab initio density functional theory, Phys. Rev. B, 90 (2014) 235301.
[68] E.A. Fitzgerald, A.Y. Kim, M.T. Currie, T.A. Langdo, G. Taraschi, M.T. Bulsara, Dislocation dynamics in relaxed graded composition semiconductors, Mater. Sci. Eng. B, 67 (1999) 53.
[69] A.Y. Kim, W.S. McCullough, E.A. Fitzgerald, Evolution of microstructure and dislocation dynamics in $In_xGa_{1-x}P$ graded buffers grown on GaP by metalorganic vapor phase epitaxy: Engineering device-quality substrate materials, J. Vac. Sci. Technol. B, 17 (1999) 1485.
[70] N.J. Quitoriano, E.A. Fitzgerald, Relaxed, high-quality InP on GaAs by using InGaAs and InGaP graded buffers to avoid phase separation, J. Appl. Phys., 102 (2007) 033511.

ACCEPTED MANUSCRIPT

Pursuant to the DOE Public Access Plan, this document represents the authors' peer-reviewed, accepted manuscript. The published version of the article is available from the relevant publisher.

ACCEPTED MANUSCRIPT

- $CuPt_B$ atomic ordering exists and affects glide energetics in GaAsP graded buffers
- The threading dislocation density rises throughout the buffer from 10^6 to 10^7 cm^{-2}
- The TDD is not correlated with glide plane switches, but is with the surface
- Dual variant $CuPt_B$ ordering is observed in GaAsP on Si substrates
- Dual- and single- variant ordering have different impacts on dislocation glide

ACCEPTED MANUSCRIPT

Pursuant to the DOE Public Access Plan, this document represents the authors' peer-reviewed, accepted manuscript. The published version of the article is available from the relevant publisher.